Observation of charge ordering by Raman scattering in $Nd_{0.5}Ca_{0.5}MnO_3$ thin films

2006 J. Phys.: Condens. Matter 18 7193

(http://iopscience.iop.org/0953-8984/18/31/014)

INSTITUTE OF PHYSICS PUBLISHING JOURNAL OF PHYSICS: CONDENSED MATTER

J. Phys.: Condens. Matter **18** (2006) 7193–7202 doi:10.1088/0953-8984/18/31/014

Observation of charge ordering by Raman scattering in $Nd_{0.5}Ca_{0.5}MnO_3$ thin films

S Charpentier, M Gill-Comeau, S Jandl and P Fournier

Regroupement québécois sur les matériaux de pointe, Département de physique, Université de Sherbrooke, Sherbrooke, QC, J1K 2R1, Canada

Received 7 June 2006, in final form 29 June 2006
Published 21 July 2006
Online at stacks.iop.org/JPhysCM/18/7193

Abstract

We report on the first observation by Raman scattering of charge ordering in thin films of $Nd_{0.5}Ca_{0.5}MnO_3$. We observe the emergence of additional phonon excitations at low temperature that confirms the structural transition accompanying the charge ordering. The properties of our defect-free $Nd_{0.5}Ca_{0.5}MnO_3$ thin films are very similar to those of the single crystals. This behaviour appears to be different from previous Raman reports on $Pr_{0.5}Ca_{0.5}MnO_3$ and $La_{0.5}Ca_{0.5}MnO_3$ thin films. We speculate that the different growth conditions, in particular our higher substrate temperature, are responsible for such a difference.

1. Introduction

Substitution of the rare-earth ion R^{3+}, by a divalent cation A^{2+} in $R_{1-x}A_xMnO_3$ (R = lanthanides and A = Ba, Sr, or Ca), generates Mn^{4+} ions leading to double-exchange interactions with a reduction of Jahn–Teller-type distortions [1–3]. The electrical and magnetic properties of doped manganites are controlled by the amount of doping and the tolerance factor [4]. Remarkably, paramagnetic–insulator, ferromagnetic–metallic, and charge ordered–insulator temperature-dependent phase transitions are induced in the doped manganites. A colossal negative magnetoresistance, which has attracted increasing interest in the last decade [5], is observed near either the concomitant paramagnetic insulator–ferromagnetic metallic phase transition [6] or the ferromagnetic metallic–charge ordered insulator transition [7]. The Mn–O–Mn bond length and angle are modified by the Mn^{3+}/Mn^{4+} distribution, while the charge transfer from an occupied Mn^{3+} e_g orbital to an adjacent Mn^{4+} unoccupied e_g orbital depends strongly on the MnO_6 octahedra tilts and Jahn–Teller distortions. Recent theoretical modelling has been centred on phase separation [8], confirming that electron-rich ferromagnetic and electron-poor antiferromagnetic domains can occur in charge-ordered phases [9].

At low temperatures, ordering of the two Mn^{3+} and Mn^{4+} sub-lattices develops with the electrons localized in real space. This phenomenon is optimized in the $x \sim 0.5$

doped manganites, since the carriers and the Mn^{3+}/Mn^{4+} ordering can become commensurate. Orbital ordering with CE-type antiferromagnetism is also observed in the doped manganites [10], either concomitant with the charge ordering (e.g. in $Nd_{0.5}Sr_{0.5}MnO_3$) or at lower temperatures (e.g. in $Nd_{0.5}Ca_{0.5}MnO_3$). The transition from the ferromagnetic metallic phase to the antiferromagnetic insulating charge-and-orbital-ordered phase with a Néel temperature (T_N) and a charge-ordering temperature (T_{co}) in the range 150–250 K was first observed in $La_{0.5}Ca_{0.5}MnO_3$ (LCMO) with the formation of a superstructure (space group $P2_1/m$) [11]. In such a system, the *a* lattice parameter of $LaMnO_3$ (*Pnma* unit cell) is doubled and the charge ordering develops in the *ac* planes at $T < T_N \sim 160$ K. Each Jahn–Teller distorted $Mn^{3+}O_6$ octahedron becomes surrounded by four undistorted $Mn^{4+}O_6$ octahedra and vice versa with rows of one type of octahedra aligned along the *b* axis.

Compared to the bulk, the manganite thin-film properties are modified due to the strains imposed by the substrate [12]. A highly strained regime located close to the substrate is followed by a more relaxed one above it with possible changes in crystalline symmetry. In-plane and out-of-plane lattice parameters are usually affected by the substrate due to lattice mismatch and alteration of Mn–O–Mn angles and Mn–O distances. For instance, $Nd_{0.5}Ca_{0.5}MnO_3$ (NCMO) films are under tensile stress on a $SrTiO_3$ (STO) substrate, with the lattice parameters expanding in the plane and contracting in the growth direction, in contrast to films under compressive stress on a $LaAlO_3$ (LAO) substrate [12]. Grown on the (100) STO-and (100) LAO-oriented planes, the NCMO orthorhombic (*Pmma* space group) films are single phase with either their [010] axis perpendicular to the STO substrate or their [101] axis perpendicular to the LAO substrate [13]. Transport properties of $Nd_{0.5}Ca_{0.5}MnO_3$ strained thin films, studied by Buzin *et al* [14], suggest that, for small film thicknesses (∼670 Å) the Mn–O bond elongations prevail, favouring the Jahn–Teller distortions and consequently the charge-orbital ordering. For large thicknesses (∼2000 Å), the Mn–O–Mn bond angles are flattened, facilitating the insulator-to-metal transition under a 7 T magnetic field, in contrast to ∼12–20 T in bulk $Nd_{0.5}Ca_{0.5}MnO_3$ [15].

Raman spectroscopy has proved its efficiency in the microscopic characterization of the mixed-valence manganites with the detection of the oxygen partial phonon density of states and phase separation [16, 17]. Abrashev *et al* [18] have studied the charge and orbital ordered state in $La_{0.5}Ca_{0.5}MnO_3$ by Raman spectroscopy. They observed that the new activated Raman modes, below $T \sim 150$ K, in the antiferromagnetic insulating ordered state were enhanced when excited with laser energies close to the Jahn–Teller gap ∼1.9 eV. These intense modes could be assigned in comparison with layered manganites and undoped $RMnO_3$ (R = La, Y). $Nd_{0.5}Sr_{0.5}MnO_3$ has also been studied by Raman spectroscopy [19–22]. In particular, Asselin *et al* [22] have shown that the Raman-active phonons of a single crystal of $Nd_{0.5}Sr_{0.5}MnO_3$ retrace the evolutions between the paramagnetic, ferromagnetic, A-type antiferromagnetic and CE-type antiferromagnetic charge and orbital ordering phase transitions. Recently, Jandl *et al* [23] have studied bulk $Nd_{0.5}Ca_{0.5}MnO_3$ phase transitions in the paramagnetic, charge-ordered ($T_{co} \sim 250$ K) and antiferromagnetic orbital-ordered ($T_N \sim 160$ K) regimes by the micro-Raman technique. At $T < T_N$, the CE-type phase dominates and 20 Raman-active modes have been detected and compared to $NdMnO_3$ [24], $CaMnO_3$ [25], $Nd_{0.5}Sr_{0.5}MnO_3$ [22] and $La_{0.5}Ca_{0.5}MnO_3$ [26] low-temperature phonon frequencies. The persistence of high-temperature ferromagnetic and A-type antiferromagnetic phase phonons corroborates phase separation. In addition to $La_{0.5}Ca_{0.5}MnO_3$, $Nd_{0.5}Sr_{0.5}MnO_3$ and $Nd_{0.5}Ca_{0.5}MnO_3$ identical crystalline structures, phonon symmetries and MnO_6 octahedra stretching, bending and tilting frequencies in the CE-type phase have indicated the development of coherent cooperative Jahn–Teller distortions as well as strong similarities in the charge and orbital orders of Ca-and Sr-doped manganites.

Raman studies of charge and orbital ordering in manganite thin films are somehow contradictory with respect to studies of single crystals. In the case of $Pr_{0.5}Ca_{0.5}MnO_3$ thin films grown on STO and LAO substrates, no significant change, except in the phonon intensities, is reported between room temperature and $T = 78$ K spectra [27], in contrast to the temperature evolution of the bulk $Pr_{0.5}Ca_{0.5}MnO_3$ Raman spectra [28]. In the Raman study of $La_{0.5}Ca_{0.5}MnO_3$ thin films (2000–3000 Å) grown on LAO (001) and STO (001) [29], low-temperature spectra do not correspond to the charge and orbital excitations in bulk single crystals [26]. Moreover, the phonon frequencies corresponding to the high-temperature paramagnetic phase observed at 425, 446, 469 and 690 cm^{-1} for LCMO/LAO thin films and 500 and 690 cm^{-1} for LCMO/STO thin films [29] do not match those observed at 487, 516, 601 and 643 cm^{-1} in bulk $La_{0.5}Ca_{0.5}MnO_3$ [26].

In this paper, we present a study of $Nd_{0.5}Ca_{0.5}MnO_3$ thin films deposited on LAO and STO substrates using transport properties and Raman-active modes under a microscope focusing on ~ 3 μm diameter areas. We have used the 632.8 nm (1.96 eV) He–Ne laser line so that the phonon intensities become resonantly enhanced as predicted around 1.9 eV [27]. Our objectives are (i) to determine if the transport measurements and Raman-active excitations in $Nd_{0.5}Ca_{0.5}MnO_3$ thin films reflect the evolution of the multiple phase transitions between room temperature and 5 K, (ii) to compare the properties of $Nd_{0.5}Ca_{0.5}MnO_3$ thin films and single crystals and evaluate the quality of the films; and (iii) to detect if phase separation develops in thin films at various temperatures, as inferred by recent models [30, 31].

2. Experiments

$Nd_{0.5}Ca_{0.5}MnO_3$ (NCMO) thin films were grown by pulsed laser ablation deposition on $LaAlO_3$ (LAO) and $SrTiO_3$ (STO) [100] substrates with two different thicknesses: $\sim$200 and 2000 Å. The films were all grown at a substrate temperature $T_{subst} = 820\,^{\circ}C$ for 2 and 20 min, respectively, in 400 mTorr of molecular oxygen with a repetition rate of 10 Hz and an estimated growth rate of 1.7 Å s^{-1}. The growth was followed by an *in situ* fast cooling ($\sim 40\,^{\circ}C\ min^{-1}$) and a post-annealing step for 15 min at 400 °C in 400 Torr of O_2. Such conditions, in particular growth at a temperature as high as 820 °C, are known to lead to weak magnetoresistance at low temperature [32]. The films were then checked by x-ray diffraction (Cu Kα with $\lambda = 1.5406$ Å) to confirm their orientation and their actual lattice parameters. Resistivity was measured using a physical properties measurement system (PPMS) from Quantum Design using a conventional four-probe technique on the same exact film that was then measured by Raman scattering (see below). The resistivity was measured at zero field and 9 T while cooling and then warming. A few films were also measured with different thermal and field cycling, and also at fixed temperature as a function of field for comparison with the literature.

Micro-Raman spectra were measured in the backscattering configuration using a He–Ne laser (632.8 nm) and a Labram-800 Raman microscope spectrometer equipped with a 50x objective, an appropriate notch filter and a nitrogen-cooled CCD detector. The thin films were mounted on the cold finger of a micro-Helium Janis cryostat perpendicular to the incident radiation, and the laser power was kept at 0.8 mW to avoid local heating. A_g and B_{2g} Raman-active phonons were detected in the *Pmma* simplified space group symmetry.

3. Results and discussion

Figure 1 presents the x-ray diffraction pattern of our 2000 Å thin films on both substrates. These spectra in a limited angular range of interest confirm the (101) and the (010) orientation

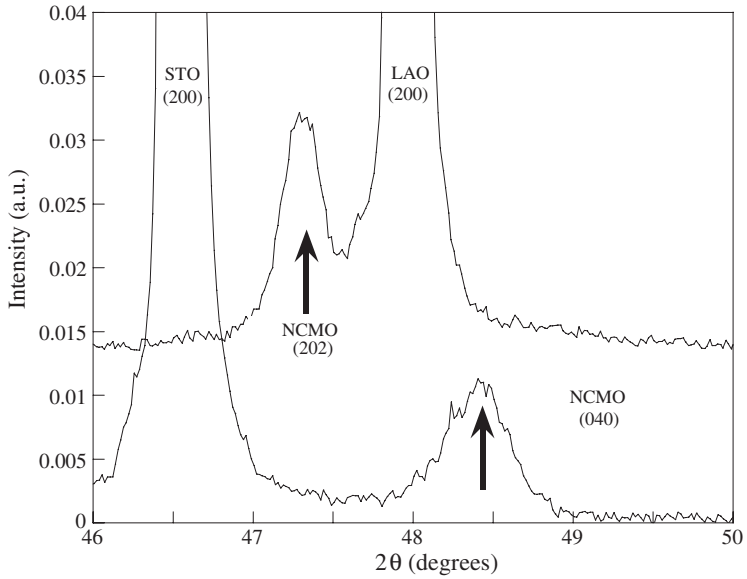

Figure 1. X-ray diffraction pattern at room temperature of the 2000 Å NCMO thin films on $SrTiO_3$ (STO) and $LaAlO_3$ (LAO) around 47°.

of the films on LAO and STO substrates, respectively.[1] The lattice parameters extracted from these spectra correspond closely to those reported in the literature for thin films ($a \sim b = 5.338$ Å, $c = 7.53$ Å) [14, 32] and differ from the bulk values [33] because of strain effects [12, 32]. Figure 2 presents the temperature dependence of the resistance of our thin films, noting the log scale on the vertical axis. At zero field, the resistance diverges quickly at low temperature to become immeasurable below ∼100 K. This divergence, although slightly different from the behaviour in single crystals [33], is quite characteristic of previous data on thin films [12, 14, 32]. Using the $\ln(R)$ versus $1000/T$ plot, we can also identify the transition through T_{co} as an S-shaped anomaly at roughly $1000/T \sim 4.55$ (close to the bulk $T_{co} \sim 240$ K [33]). This feature can be further evidenced as a peak at T $\Delta T_{co} = 240$ K in the first derivative $\mathrm{d}\ln(R)/\mathrm{d}(1000/T)$, as shown in the inset. We should mention here that a similar peak, although much sharper, is expected from the single-crystal data that show a sudden upturn of resistivity at T_{co} (see figure 6 of [33]). In a large magnetic field of 9 T, our NCMO thin films show a large magnetoresistance, comparable to that reported in [12, 14, 32] on similar films grown at similar temperatures. We want to underline here that, in a few cases, the films showed little magnetoresistance up to 9 T, indicating a much larger CO (charge-ordered) melting field than usual. The origin of such properties on films as thick as 2000 Å is still under investigation.

In $Nd_{0.5}Ca_{0.5}MnO_3$, the most significant difference between room temperature and low temperature is governed by the Mn–O bonds. At room temperature, while the oxygen octahedra are almost undistorted with six approximately equal Mn–O bond lengths, below T_N the two Mn–O distances along the b-axis become shorter than the four a–c plane Mn–Os, resulting in Jahn–Teller distortions [32].

[1] The width of the x-ray diffraction peaks are resolution limited. X-ray diffraction was used here only to assess thin-film orientation, the lattice parameters and the absence of secondary phases. More extensive studies are underway on that matter, but they do not indicate major changes in the width of the peaks with respect to previous publications (see [14]).

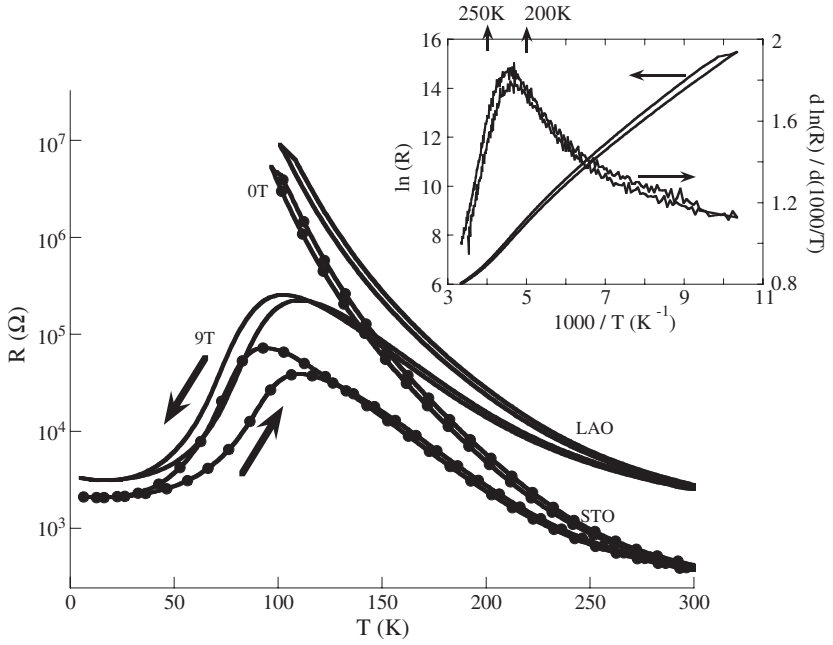

Figure 2. Resistance as a function of temperature for the 2000 Å NCMO thin films on STO (solid circles and lines) and LAO (solid lines) at 0 and 9 T. Arrows indicate the temperature sweep directions. Inset: $\ln(R)$ versus $1000/T$ at 0 T for NCMO on STO and its first derivative, showing a peak at $T \sim T_{co}$.

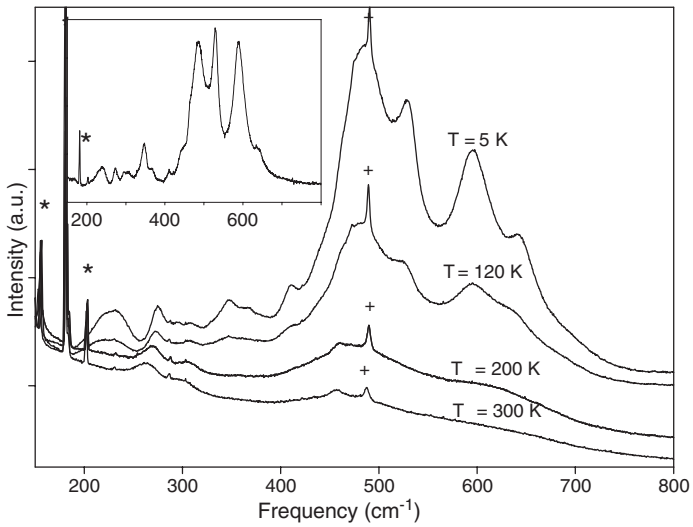

Figure 3. 2000 Å NCMO/LAO thin film Raman active phonons as a function of temperature. Inset: $Nd_{0.5}Ca_{0.5}MnO_3$ single crystal Raman active phonons at $T = 5$ K. $*$ and $+$ indicate plasma laser lines and $LaAlO_3$ phonons respectively.

3.1. NCMO on LAO

Raman spectra, at various temperatures, of 2000 and 200 Å NCMO/LAO thin films are presented in figures 3 and 4, respectively. At 300 K, the $Nd_{0.5}Ca_{0.5}MnO_3$ space group

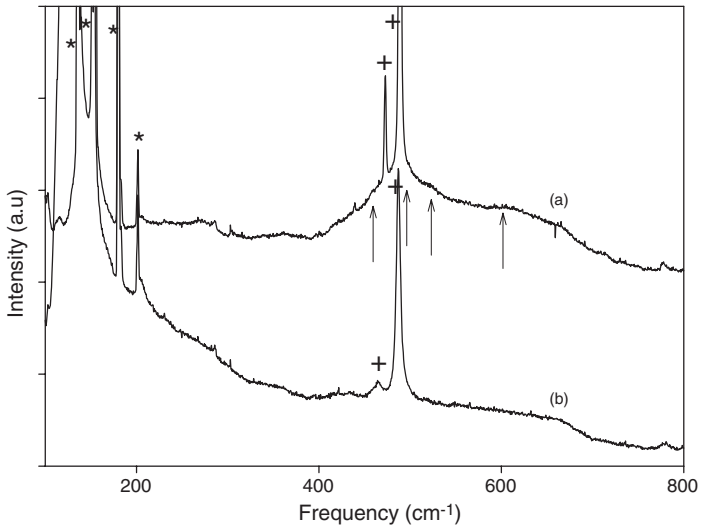

Figure 4. 200 Å NCMO/LAO thin film Raman-active phonons at $T = 5$ K (a) and 300 K (b): $*$, $+$ and $\uparrow$ indicate plasma laser lines, $LaAlO_3$ phonons and thin-film phonons, respectively.

is *Pnma* and three excitations are observed at around 264, 300 and 458 cm^{-1} in the 2000 Å NCMO/LAO thin-film paramagnetic phase (figure 3). These correspond to the $\sim$265 cm^{-1} (A_g), 290 cm^{-1} (A_g) and 440 cm^{-1} (B_{2g}) excitations observed in the single-crystal paramagnetic phase [23]. Such bands have been associated with the insulating high-temperature phase of the manganite's rotation-like mode ($\sim$250 cm^{-1}) which measures the rotational and the Jahn–Teller ($\sim$450 cm^{-1}) distortions, respectively [17]. Similarly to the single crystal, and on cooling down the thin film below $T_{co} \sim 240$ K, the space group remains *Pnma* and new broad excitations develop at around 500 and 610 cm^{-1} (figure 3), delineating the charge-order regime.

Below $T_N \sim 160$ K, $Nd_{0.5}Ca_{0.5}MnO_3$ adopts the CE-type antiferromagnetic monoclinic symmetry ($P2_1/m$) [20], rendering many phonons Raman active. Excitations around 227, 272, 294, 305, 346, 366, 408, 445, 462, 480, 527, 593, and 639 cm^{-1} are detected (figure 3). These correspond to A_g and B_{2g} Raman-active phonons observed below T_N in the $Nd_{0.5}Ca_{0.5}MnO_3$ single crystal [20] measured in the same configuration (figure 3 inset). The NCMO/LAO thin-film phonons are broader than those of the single crystal: for the 272 and 593 cm^{-1} phonons, we obtain respectively 17 and 30 cm^{-1} for the films, while this is 10 and 25 cm^{-1} for the single crystal. Their frequencies are slightly shifted by $\sim \pm 1$ cm^{-1}, except for the 593 cm^{-1} phonon ($\sim +5$ cm^{-1}). This particular excitation is associated with the in-phase stretching of oxygen atoms in the *ac* plane [18]. The observation of these additional phonons only at low temperature in the thin films confirms the presence of the CE-type antiferromagnetic and the orbital ordering transitions, similarly to the single crystal and in clear contrast to previous Raman studies of $Pr_{0.5}Ca_{0.5}MnO_3$ and $La_{0.5}Ca_{0.5}MnO_3$ thin films [27, 29]. These previous reports showed important discrepancies with the single-crystal measurements [26, 28]. In figure 4, Raman excitations of NCMO/LAO 200 Å thin film at $T = 5$ K compared to the $T = 300$ K spectrum indicate the presence of the CE-type strong excitations (figure 4 arrows) broadened by interface strains and emerging from the background despite the small thickness of the film. The ability of the charge and orbital ordering to develop in small-thickness NCMO/LAO thin films is thus also confirmed.

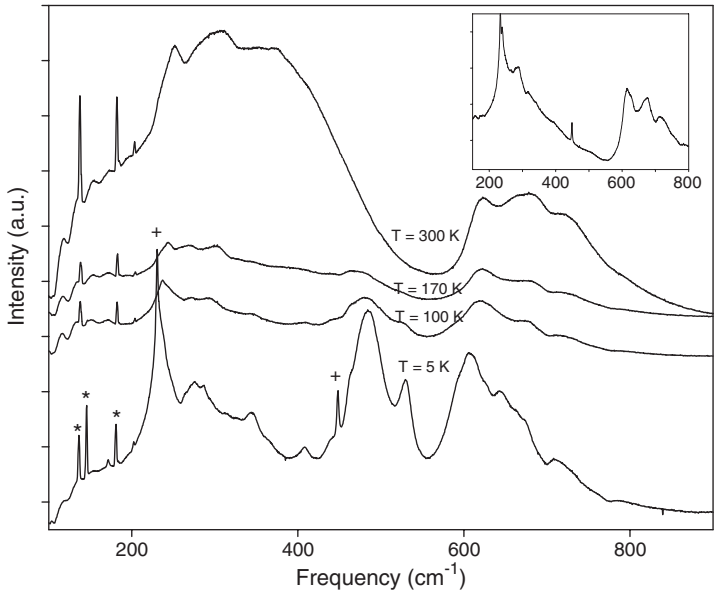

Figure 5. 2000 Å NCMO/STO thin-film Raman-active phonons as a function of temperature. Inset: $SrTiO_3$ substrate Raman-active phonons at $T = 5$ K.

3.2. NCMO on STO

In figure 5, Raman excitations of 2000 Å NCMO/STO thin film at different temperatures are shown. The $SrTiO_3$ substrate Raman excitations are visible in the spectra. Although the film and substrate spectra are identical at 300 K, the spectra differ at low temperatures, indicating the occurrence of the CE-type antiferromagnetic and the orbital ordering transitions with the strong characteristic excitations emerging once again from the (substrate) background. These excitations correspond closely to those observed with NCMO/LAO, at around 230, 272, 346, 366, 408, 445, 464, 480, 528, 593, and 639 cm^{-1} at $T = 8$ K. The NCMO/STO thin-film orientation, with the [010] axis perpendicular to the substrate, allows distinct observations of the A_g (272, 346, 336, 528, and 593 cm^{-1}) and B_{2g} (230, 408, 445, 464, 480, and 639 cm^{-1}) phonons in the y(xx)y and y(xz)y Raman configurations, respectively (figures 6(a) and (b)). The perfect correspondence between the thin film and the single-crystal phonon symmetries is an indication of the strain's minor role in the overall film symmetry and orientation. Finally, the excitations of the 200 Å NCMO/STO thin film are not strong enough, at all temperatures, to be discriminated from the substrate.

The overall evolutions, as a function of temperature, of the NCMO/LAO and NCMO/STO thin films and $Nd_{0.5}Ca_{0.5}MnO_3$ single-crystal phonons are very similar. Between room temperature and T_N, the five observed phonons are induced by dynamical incoherent Jahn–Teller distortions. They persist below T_N, indicating the occurrence of phase separation at low temperature [16]. At $T_{co} < T < T_N$, phonon excitations at around the 475 and 600 cm^{-1} bending and stretching bands are broad and disorder-induced, indicating spatially incoherent Jahn–Teller distortions. Below T_N, with charge and complete orbital orderings, these excitations strengthen and sharpen, becoming Raman allowed following the occurrence of static and coherent Jahn–Teller distortions. In the CE-type antiferromagnetic phase, many additional Raman excitations have their intensity strongly enhanced as the temperature is lowered. These

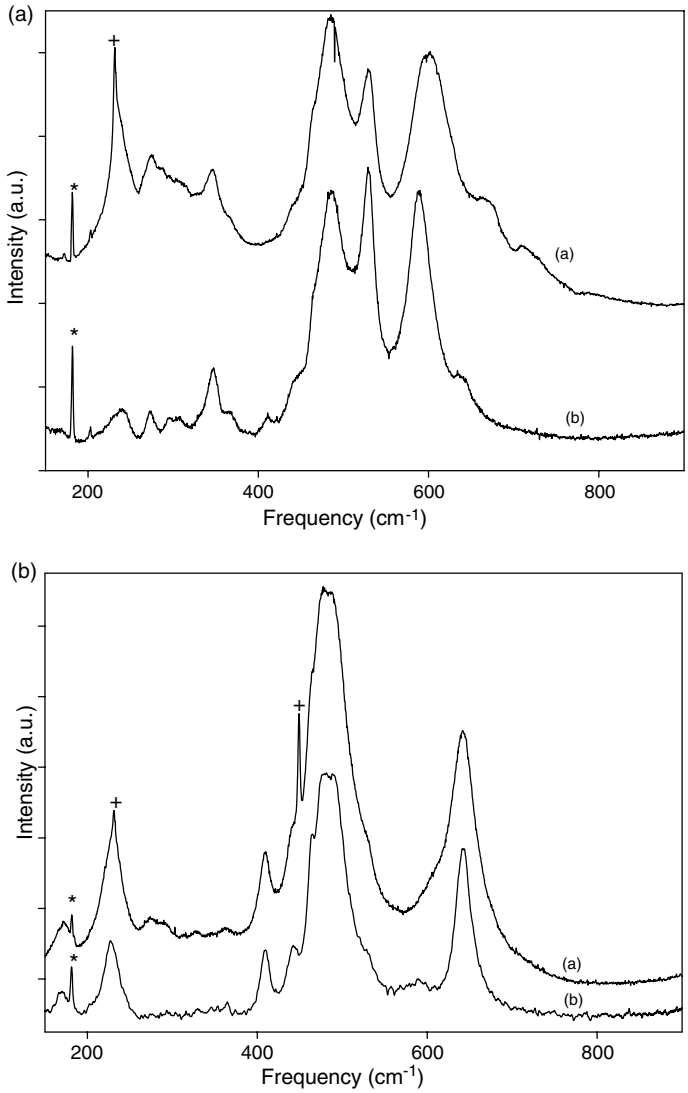

Figure 6. 2000 Å NCMO/STO thin film (a) and $Nd_{0.5}Ca_{0.5}MnO_3$ single-crystal (b) A_g Raman-active phonons at $T = 5$ K. 2000 Å NCMO/STO thin film (a) and $Nd_{0.5}Ca_{0.5}MnO_3$ single-crystal (b) B_{2g} Raman-active phonons at $T = 5$ K.

are compatible with charge and orbital ordering, as in $Nd_{0.5}Sr_{0.5}MnO_3$ and $La_{0.5}Ca_{0.5}MnO_3$, delineating the sample's structural evolutions [22, 26].

3.3. Role of defects and the robustness of CO

In contrast to the $Pr_{0.5}Ca_{0.5}MnO_3$ [27] and $La_{0.5}Ca_{0.5}MnO_3$ [29] thin films grown on STO and LAO substrates where orbital ordering *is not detected* by Raman scattering, such a low-temperature phase is clearly observed in our NCMO/LAO and NCMO/STO thin films as their counterpart in single crystals [23] with new modes appearing as the symmetry of the

crystal structure is lowered through the transition. Furthermore, no local modes that would be associated with defects or oxygen non-stoichiometry are observed in our NCMO/LAO and NCMO/STO thin films, in contrast also to a few unidentified excitations in the same previous Raman studies of PCMO and LCMO thin films [27, 29]. We interpret this result as a clear indication that our growth parameters, in particular the higher substrate temperature during deposition, improve the stoichiometry and remove undesirable defects. We should recall here that the PCMO films studied in [27] were grown at 725 °C compared to our $T_{subst} = 820$ °C. Finally, the strains caused by the lattice–substrate mismatch are not severe and are manifested mainly in minor phonon band broadening. They are, however, effective enough to facilitate the insulator-to-metal transition under a 9 T magnetic field, in contrast to ∼12–20 T in bulk $Nd_{0.5}Ca_{0.5}MnO_3$ [15].

Our thin-film properties possibly stem from their particularly high quality, being defect free as demonstrated by the absence of local modes, with minimum strain resulting only in slight phonon shifts and broadening. We suspect that the structural transition accompanying the antiferromagnetic, charge and orbital long-range ordering is very sensitive to defects that could *impose* local tilting of the MnO_6 octahedra and would be detrimental to long-range structural order. The short-range order resulting from the presence of even a very small amount of defects leads to a complete suppression of the expected phonon excitations usually observed in well-ordered and defect-free single crystals. It is interesting to note also that little can be said on the possible observation of a real CO phase based only on magnetoresistance (MR) and x-ray diffraction results. In fact, if one compares previously published data [14] and our results, we conclude that the transport properties are quite similar for NCMO films grown in *the exact same conditions*. Only Raman scattering appears to be a stringent test for the presence of charge ordering over a significant part of the sample. Since our films were grown at a higher temperature than the PCMO films studied previously [27], it suggests that the most robust CO state is achieved for a high substrate temperatures.

Here, there is one important comment that we can make on the criterion used to assess the quality of the thin films of charge-ordered materials. In [14], it is mentioned that the optimal growth conditions were determined by comparing and *maximizing* the magnetoresistance observed at low temperature (∼75 K) for films made under different growth conditions (temperature of substrates in [14]). The authors concluded that the optimal growth substrate temperature is ∼730 °C. Although it might be justified to maximize the MR from a technological point of view, such a criterion completely neglects the fact that the CO melting field is supposed to be ∼12–20 T [15], which means that one should require the magnetoresistance at fields of the order of 9 T to be as small as possible in order for the films to approach single-crystal quality with robust CO. Obviously, growth at temperatures higher than those reported previously with PCMO [14], and used in this present report with NCMO, seems to promote properties approaching nearer to those of the CO single crystals. Similar studies of Raman scattering in thin films of PCMO and LCMO as a function of the growth parameters could clarify this whole issue. This work is in progress.

4. Summary

In summary, we report the first observation of charge ordering by Raman scattering in thin films of $Nd_{0.5}Ca_{0.5}MnO_3$. We observe the emergence of additional phonon excitations at low temperature that confirms the structural transition accompanying the charge ordering. Thus, the properties of our defect-free NCMO thin films are approaching those of the single crystals. This behaviour appears to be different from previous Raman reports on $Pr_{0.5}Ca_{0.5}MnO_3$ and $La_{0.5}Ca_{0.5}MnO_3$ thin films. We speculate that the different growth conditions, in particular our

higher substrate temperature, are responsible for such difference. This study demonstrates that Raman scattering is a stringent test of the quality of charge-ordered materials.

Acknowledgments

We thank J Laverdière and M Iliev for many discussions, and S Pelletier and M Castonguay for technical support. This work was supported by the Natural Science and Engineering Research Council of Canada, Canada Foundation for Innovation, the Canadian Institute for Advanced Research and *Fonds Québécois de la Recherche sur la Nature et les Technologies*.

References

[1] Zener C 1951 *Phys. Rev.* **82** 403
[2] Khomskii D I and Sawatzky G A 1997 *Solid State Commun.* **102** 87
[3] Jim S, Tiefel T H, McCormack M, Fastnacht R, Ramesh R and Chen L H 1994 *Science* **264** 413
[4] Woodward P M, Vogt T, Cox D E, Arulraj A, Rao C N R, Karen P and Cheetham A K 1998 *Chem. Mater.* **10** 3652
[5] Ramirez A P 1997 *J. Phys: Condens. Matter* **9** 8171
[6] Coey J M D, Viret M and von Molnar S 1999 *Adv. Phys.* **48** 167
[7] Uehara M, Mori S, Chen C H and Cheong S W 1999 *Nature* **399** 560
[8] Dagotto E, Burgy J and Moreo A 2003 *Solid State Commun.* **126** 9
[9] Salamon M B and Jaime M 2001 *Rev. Mod. Phys.* **73** 583
[10] Rao C N R, Arulraj A, Cheetham A K and Raveau B 2000 *J. Phys.: Condens. Matter* **12** R83
[11] Radaelli P G, Cox D E, Marezio M and Cheong S W 1997 *Phys. Rev.* B **55** 3015
[12] Prellier W, Lecoeur Ph and Mercey B 2001 *J. Phys.:Condens. Matter* **13** R915
[13] Haghiri-Gosnet A M, Hervieu M, Simon Ch, Mercey B and Raveau B 2000 *J. Appl. Phys.* **88** 3545
[14] Rauwel Buzin E, Prellier W, Mercey B, Simon Ch and Raveau B 2003 *J. Phys.: Condens. Matter* **14** 3951
[15] Tokunaga M, Miura N, Tomioka Y and Tokura Y 1998 *Phys. Rev.* B **57** 5259
[16] Mayr M, Moreo J A, Vergés J A, Arispe J, Feiguin A and Dagotto E 2001 *Phys. Rev. Lett.* **86** 135
[17] Iliev M N, Abrashev M V, Popov V N and Hadjiev V G 2003 *Phys. Rev.* B **67** 212301
[18] Abrashev M V, Bäckström J, Börjesson L, Pissas M, Kolev N and Iliev M N 2001 *Phys. Rev.* B **64** 144429
[19] Kuroe H, Habu I, Kuwahara H and Sekine T 2002 *Physica* B **316/317** 575
[20] Choi K Y, Lemmens P, Güntherodt G, Pattabiraman M, Rangarajan G, Gnezdilov V P, Balakrishnan G, Paul D Mc K and Lees M R 2003 *J. Phys.: Condens. Matter* **15** 3333
[21] Seikh M M, Sood A K and Narayana C 2005 *Pramana* **64** 119
[22] Asselin S, Jandl S, Fournier P, Mukhin A A, Ivanov V Yu and Balbashov A M 2005 *J. Phys.: Condens. Matter* **17** 5247
[23] Jandl S, Mukhin A A, Ivanov V Yu and Balbashov A M 2006 *J. Phys.: Condens. Matter* **18** 1667
[24] Abrashev M V, Bäckström J, Börjesson L, Popov V N, Chakalov R A, Kolev N, Meng R L and Iliev M N 2002 *Phys. Rev.* B **65** 18430
[25] Granado E, Moreno N O, Martinho H, Garcia A, Sanjurjo J A, Torriani I, Rettori C, Neumier J J and Oseroff S B 2001 *Phys. Rev. Lett.* **86** 5385
[26] Abrashev M V, Bäckström J, Börjesson L, Pissas M, Kolev N and Iliev M N 2001 *Phys. Rev.* B **64** 144429
[27] Tatsi E, Papadopoulo E L, Lampakis D, Liaropakis E, Prellier W and Mercey B 2003 *Phys. Rev.* B **68** 024432
[28] Dediu V, Ferdeghini C, Matacotta F C, Nozar P and Ruani G 2000 *Phys. Rev. Lett.* **84** 4489
[29] Xiong Y M, Chen T, Wang G Y, Chen X H, Chen X and Chen C L 2004 *Phys. Rev.* B **70** 094407
[30] Dagotto E, Burgy J and Moreo A 2003 *Solid State Commun.* **126** 9
[31] Mayr M, Moreo J A, Vergés J A, Arispe J, Feiguin A and Dagotto E 2001 *Phys. Rev. Lett.* **86** 135
[32] Rauwel Buzin E, Prellier W, Simon Ch, Mercone S, Mercey B, Raveau B, Sebek J and Hejtmanek J 2001 *Appl. Phys. Lett.* **79** 647
[33] Millange F, de Brion S and Chouteau G 2000 *Phys. Rev.* B **62** 5619